Investigation of memristors' own parasitic parameters and mutual inductances between neighbouring elements of a memristor matrix and their influence on the characteristics

Valeri Mladenov
Dept. of Theoretical Electrical Engineering
Technical University of Sofia
Sofia, Republic of Bulgaria
E-mail: valerim@tu-sofia.bg

Stoyan Kirilov
Dept. of Theoretical Electrical Engineering
Technical University of Sofia
Sofia, Republic of Bulgaria
E-mail: s_kirilov@tu-sofia.bg

***Abstract* — The main purpose of the paper is to analyze the parasitic parameters and the mutual inductances between the neighboring memristors of a memristor memory matrix. An equivalent substituting circuit of two neighboring memristors with different parameters of a memristor memory matrix is given. Then the parasitic capacitance and inductance of a memristor are calculated. Three possible values of the coefficient of magnetic connection are used. A SIMULINK model of the circuit investigated is created. The basic relationships between the quantities in graphical form are presented. The main result is that the parasitic parameters do not strongly affect the memristor voltage drops at frequencies up to 2 GHz. In the end, some concluding remarks associated with the magnetic influence between the memristors of a memristor memory matrix are given.**

Keywords—titanium-dioxide memristor; parasitic parameters; mutual inductance; memristor characteristics.

I. INTRODUCTION

One of the most interesting and useful properties of the memristor is the memorizing the full amount of charge which has passed through it [1, 2, 3]. Many research investigations and simulations on this nonlinear circuit element have been made in the last few years [4, 5]. The main properties and the principle of operation of Williams's memristor have been presented [6, 7]. Some physical dependencies between the basic electrical quantities of the memristor have been shown in the literature [8, 9, 10]. As every real electric element the titanium-dioxide memristor has a parasitic capacitance and an inductance. Realized on an integrated circuit every two neighboring memristors have also mutual inductance. These parameters are dependent of the memristor chip size and the positions of the elements [10, 11, 12]. In the papers published no data on this topic have been found. The main purpose of this paper is to propose adequate substituting circuit and a suitable SIMULINK model of the neighboring memristors for further analysis [13, 14].

In Section II an equivalent substituting circuit of two neighboring memristors is proposed. The concrete values of the parasitic parameters and of the mutual inductance are calculated in Section III. The SIMULINK model based on the circuit presented and the results of the simulation realized are given in Section IV. The concluding remarks are presented in Section V.

II. EQUIVALENT SUBSTITUTING CIRCUIT OF TWO NEIGHBOURING MEMRISTORS OF A MEMRISTOR MEMORY MATRIX

The equivalent scheme of the two nearly placed on a matrix memristors is presented in Fig. 1. The capacitors C_1 and C_2 present memristor's own capacitances due to the overlapping between the memristors electrodes. The inductors L_1 and L_2 present the parasitic inductances of each of the platinum rims. The coefficient M is almost equal to each of inductances because of the full embracement of the magnetic flux by both of the platinum rims of the elements. The coefficient of magnetic influence k has a value which is very near to 1. In this investigation three values of the coefficient k are given – $k = 0.90$, $k = 0.95$ and $k = 0.99$.

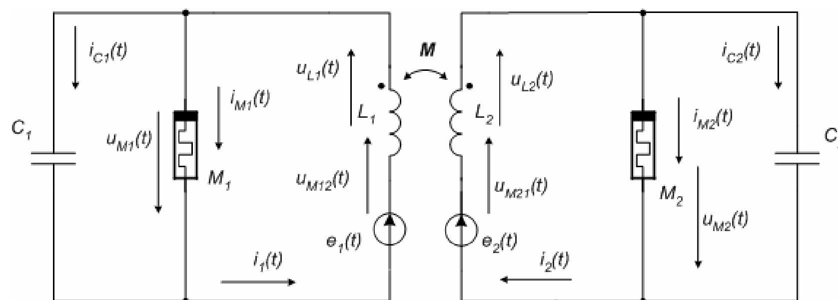

Fig. 1. Equivalent circuit of two neighboring memristors of a memory matrix

III. CALCULATION OF PARASITIC CAPACITANCES, INDUCTANCES AND MUTUAL INDUCTANCE

The capacitances C_1 and C_2 are calculated as a capacitance of a plane capacitor. The parasitic capacitance is a combination of two capacitances – those of the doped and of the undoped regions, connected in series. The values of dielectric permittivity of these two sub-layers are $\varepsilon_{r1} = 170$ and $\varepsilon_{r2} = 150$, respectively. The width of the memristor electrodes is a = 50 *nm.* The lengths of the doped and undoped regions are $D_1 = w_1$ = 1 *nm*, $D_2 = D\text{-}w_1$ = 90 *nm.* The equivalent capacitance is given with Eq. (1):

$$C_{par} = \frac{C_1 C_2}{C_1 + C_2} = \frac{\varepsilon_0 \varepsilon_{r1} \frac{a^2}{D_1} \varepsilon_0 \varepsilon_{r2} \frac{a^2}{D_2}}{\varepsilon_0 \varepsilon_{r1} \frac{a^2}{D_1} + \varepsilon_0 \varepsilon_{r2} \frac{a^2}{D_2}} \tag{1}$$

The numerical result of the parasitic capacitance of the memristor is $C_{par} = 3.10^{-16}$ *F*.

The parasitic inductance is calculated with solving of double definite integral and with using of magnetic field theory. A conductor with finite length l is disposed over the z-axis. A permanent current with intensity i flows through the wire. A current element idl is placed in the centre of a Cartesian coordinate system – Fig. 2. The induction lines of the magnetic field are concentric circles which are placed in planes parallel to the plane $x0y$.

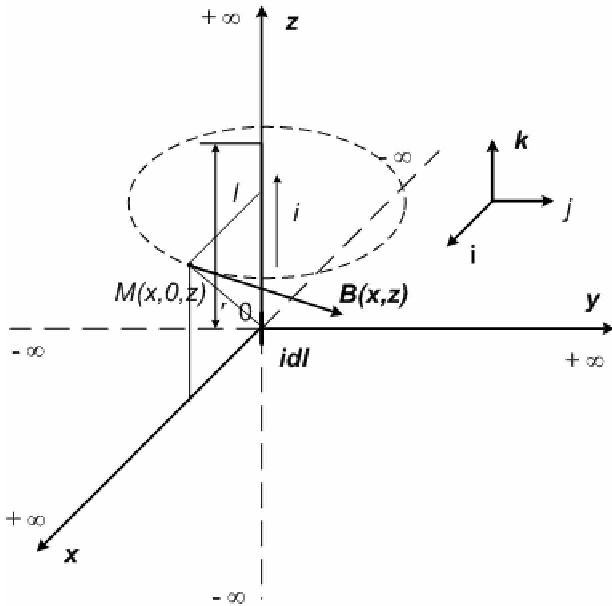

Fig. 2. Theoretical formulation for determine the coefficient of inductance of the titanium-dioxide Williams's memristor

The tangent vector to the circle ***B(x,z)*** is the vector of magnetic flux density. It is determined by the Biot-Savart law:

$$d\vec{B}(r) = \frac{\mu_0 idl}{4\pi r^2} \vec{k} \times \vec{e}_r \tag{2}$$

The radius of the sphere on which the point M lies has a length given with Eq. (3):

$$r = \sqrt{x^2 + z^2} \tag{3}$$

The single vector on the radius-vector of point M is presented with Eq. (4):

$$\vec{e}_r = \frac{x\vec{i} + z\vec{k}}{\sqrt{x^2 + z^2}} \tag{4}$$

After transformations we obtain Eq. (5):

$$d\vec{B}(x,z) = \vec{j} \frac{\mu_0 i}{4\pi} \frac{x}{(x^2 + z^2)^{\frac{3}{2}}} dz \tag{5}$$

The full magnetic flux obtained by the current element idl is presented with Eq. (6):

$$\begin{aligned} d\Phi &= \int_{-\infty}^{+\infty} \int_{0}^{+\infty} d\vec{B}(x,z) dx dz \vec{j} = \\ &= \int_{-\infty}^{+\infty} \int_{0}^{+\infty} \vec{j} \frac{\mu_0 i}{4\pi} \frac{x}{(x^2 + z^2)^{\frac{3}{2}}} dz dx dz \vec{j} = \\ &= dz \int_{-\infty}^{+\infty} \int_{0}^{+\infty} \frac{\mu_0 i}{4\pi} \frac{x}{(x^2 + z^2)^{\frac{3}{2}}} dx dz \end{aligned} \tag{6}$$

The full magnetic flux generated by the wire with length l is obtained after integration with respect to the coordinate z:

$$|\Phi| = \frac{\mu_0 i}{4} \int_0^l dz = \frac{\mu_0 i}{4} l \tag{7}$$

The inductance of the memristor is given with Eq. (8):

$$\begin{aligned} L &= \left| \frac{\Phi}{i} \right| = \left| \frac{\frac{\mu_0 i}{4} l}{i} \right| = \frac{\mu_0}{4} l = \\ &= \frac{4\pi.10^{-7}}{4}.0,03 = \\ &= 9,4248.10^{-9}\ H = 9,4\ [nH] \end{aligned} \tag{8}$$

The parasitic inductance of one memristor in the center of the memory matrix has a value of L = 9,4 *nH*.

The mutual inductance M is calculated with participation of the mutual magnetic flux between the parallel wires. Its value is near to the value of the memristor's own inductance.

The parameters of the second memristor are 5 % larger than the parameters of the first memristor:

$$C_2 = 1,05.C_1 = 1,05.3.10^{-16} = 3,15.10^{-16}\ F$$

$$L_2 = 1,05.L_1 = 1,05.9,4.10^{-9} = 9,87\ \text{n}H$$

$$e_{m1} = e_{m2} = 1\ V$$

$$R_{ON2} = 1,05.R_{ON1} = 1,05.100 = 105\ \Omega$$

$$R_{OFF2} = 1,05.R_{OFF1} = 1,05.16 = 16,8\ k\Omega$$

The mutual inductance is calculated with the use of the coefficient of magnetic connection k and the inductances of the memristors:

$$M_1 = k_1\sqrt{L_1L_2} = 0,90.\sqrt{9,4.10^{-9}.9,87.10^{-9}} = 8,67\ nH$$

$$M_2 = k_2\sqrt{L_1L_2} = 0,95.\sqrt{9,4.10^{-9}.9,87.10^{-9}} = 9,15\ nH$$

$$M_3 = k_3\sqrt{L_1L_2} = 0,99.\sqrt{9,4.10^{-9}.9,87.10^{-9}} = 9,54\ nH$$

IV. SYNTHESIS OF A SIMULINK MODEL OF THE CIRCUIT INVESTIGATED AND PRESENTATION OF THE SIMULATIONS RESULTS AT IMPULSE MODE

The SIMULINK model of the circuit investigated is presented in Fig. 3. This circuit will be used also for analysis of the equivalent circuit when the elements have manufacture tolerances of their basic parameters [11].

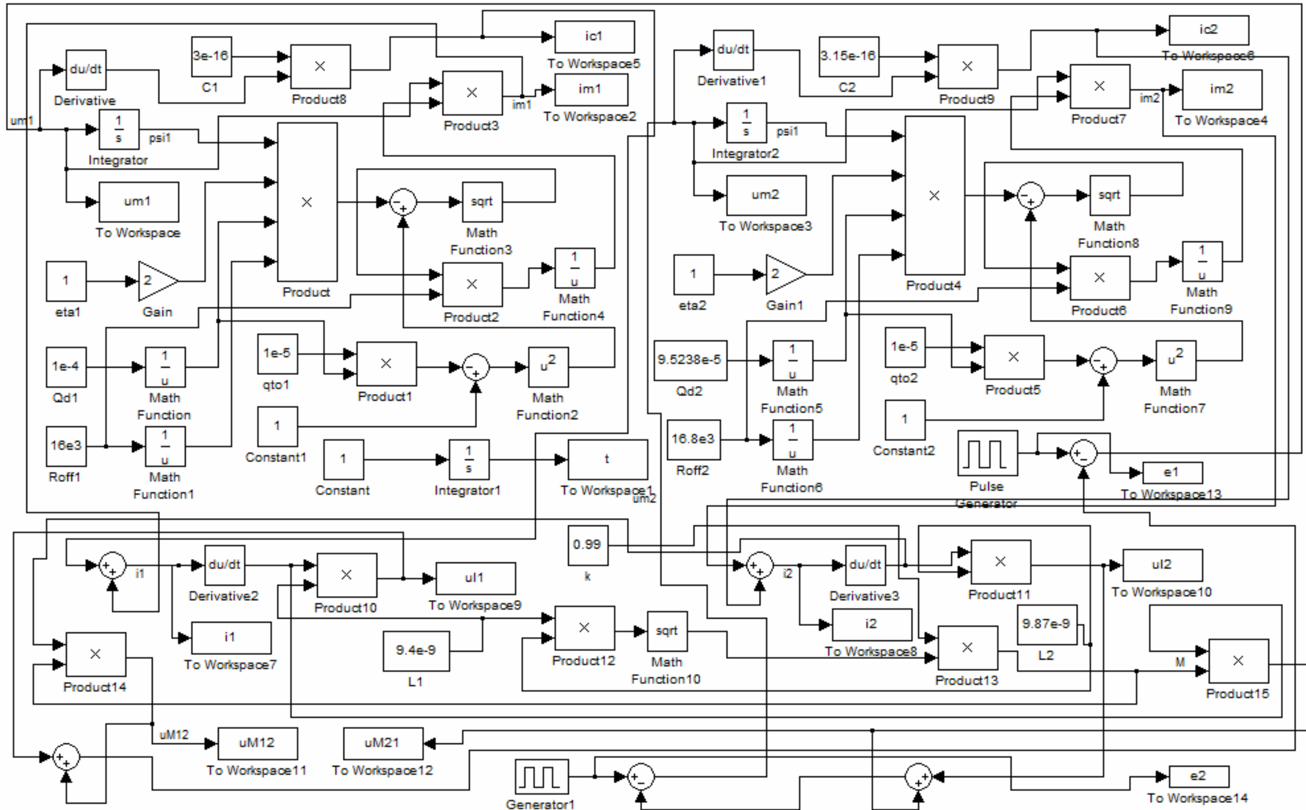

Fig. 3. SIMULINK model of the circuit investigated

The first simulation is made when only the first voltage source e_1 is switched on. The time diagram of the source voltage e_1 is presented in Fig. 4. The frequency of the signal is 2 GHz and the magnitude is 1 V.

The time diagram of mutual inductive voltage drop in inductor L_2 generated by the current i_1 is given in Fig. 5. It has a very high value and a complicated form, due to the higher harmonics of the current.

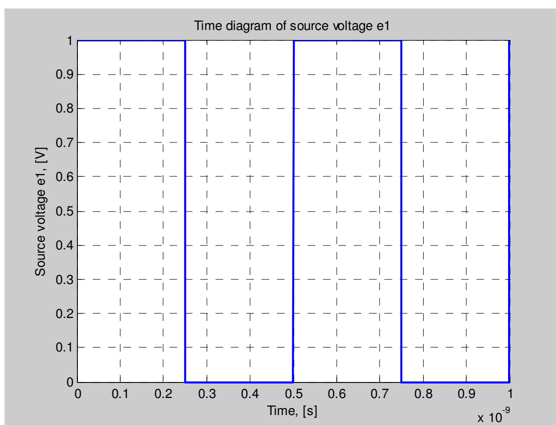

Fig. 4. Time diagram of the source voltage $e_1(t)$

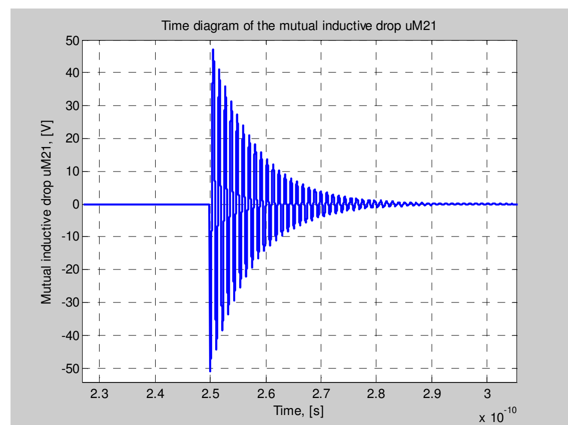

Fig. 5. Time diagram of mutual inductive voltage drop u_{M21}

The time diagram of the memristor voltage drop u_{m2} caused by the electromagnetic induction is given in Fig. 6. The voltage presented is made of short impulses with low magnitude.

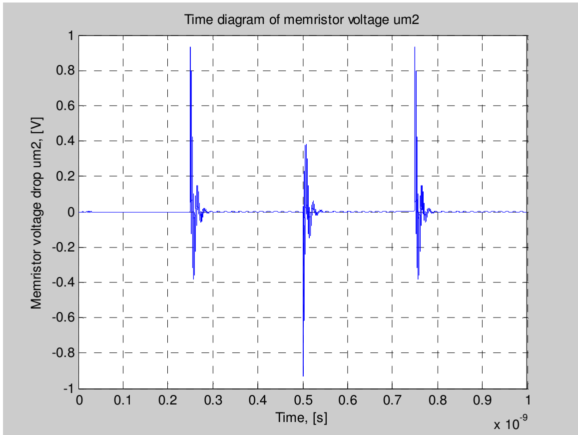

Fig. 6. Time diagram of the memristor voltage drop u_{m2}

The time diagram of the source power generated is presented in Fig. 7.

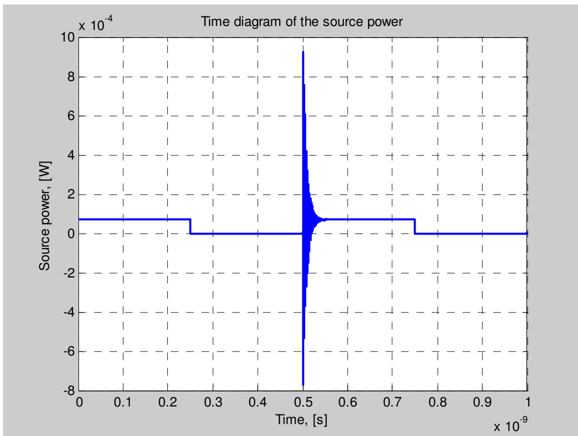

Fig. 7. Time diagram of the source power

Now we present the results of an experiment when both sources are switched on. The time diagram of source voltages is the same as the time diagram in Fig. 4. The diagram of the source current i_1 is presented in Fig. 8. Due to the transient process the plateaus of the impulses are distorted. The transient is pseudo-periodic. The maximal value of the first ricochet is about 50 % of the magnitude of the plateaus of the current pulses.

The time diagrams of the parasitic capacitance currents are shown in Fig. 9. At first glance the currents i_{c1} and i_{c2} coincide absolutely. The current impulses are with a short duration.

The memristor currents i_{m1} and i_{m2} caused by both sources are presented in Fig. 10. The time diagrams of the currents do not coincide because of the difference of the resistances of the memristors. The first current i_{m1} is higher than the current of the second memristor i_{m2} because the resistances of the second memristor are higher than these of the first element. But the shapes of the current impulses through the two memristors are the same.

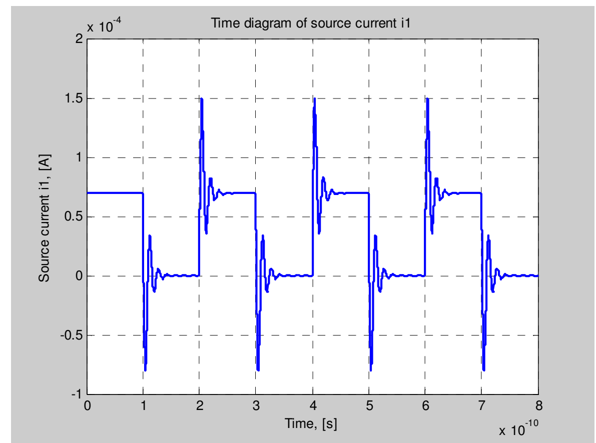

Fig. 8. Time diagram of the source current i_1

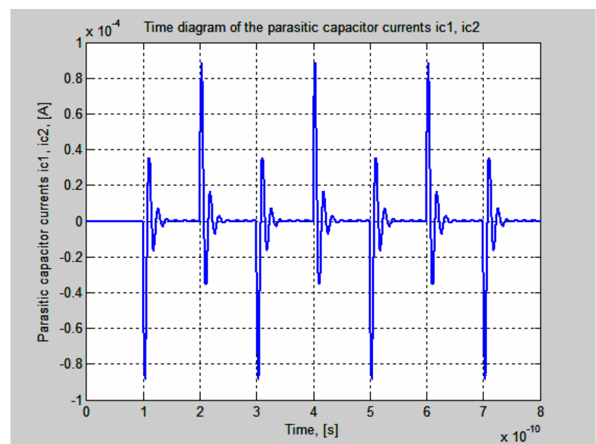

Fig. 9. Time diagrams of parasitic capacitors currents

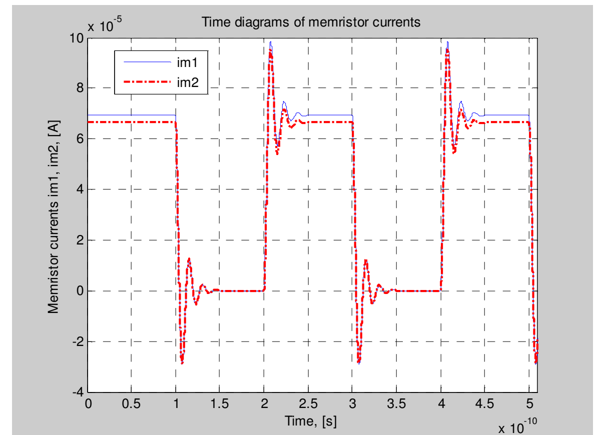

Fig. 10. Time diagrams of memristor currents i_{m1}, i_{m2}

The time diagrams of the inductive voltage drops over the inductors L_1 and L_2 are shown in Fig. 11. The shapes of the impulses are similar to that given in Fig. 9.

The voltage drops over the memristors are presented in Fig. 12. It is clear that the plateaus of the voltage impulses are distorted. The first ricochet of the impulses is about 40 percents of the plateau of the voltage drop pulses. There are

no losses of information. The pulses of the logical unity and of the logical zero are clearly expressed.

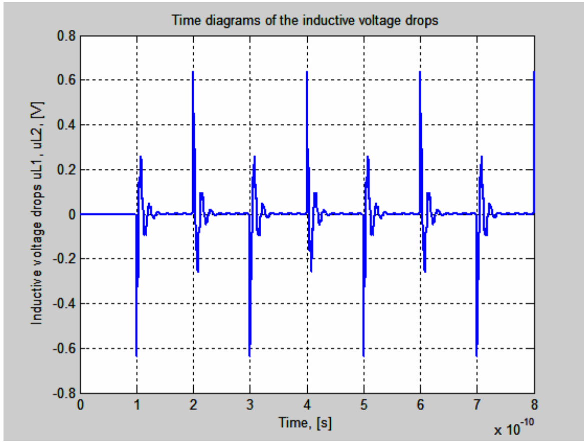

Fig. 11. Time diagrams of the inductive voltage drops u_{L1}, u_{L2}

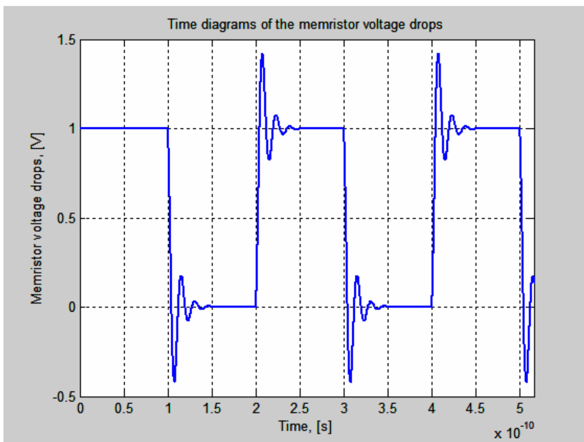

Fig. 12. Time diagrams of memristors voltage drops

The time diagram of the mutual inductive voltage drops are calculated at three different possible values of the coefficient of magnetic influence *k*. The first diagram for coefficient $k = 0.90$ is shown in Fig. 13. The detailed diagram of the mutual inductive voltage drops shows that the two voltage drops are almost similar but do not fully coincide.

The second time diagram is created for $k = 0.95$ and it is presented in Fig. 14. It is obvious that the mutual inductive voltage drops have higher magnitude than the magnitude of the first case.

The third case is when the magnetic influence between the two memristors is very strong and $k = 0.99$. The time diagram of the mutual inductive voltage drops is presented in Fig. 15. The shape of the signals is more complicated and the magnitudes in the beginning of the transient are higher than the magnitudes of the mutual inductive voltage drops in the two previous cases. The power transmitted form the first memristor to the second one is due to the mutual inductive connection between the two parasitic inductances. The time diagrams of the power transmitted from the one memristor to the other and vice versa are shown in Fig. 16. The two time diagrams coincide almost entirely.

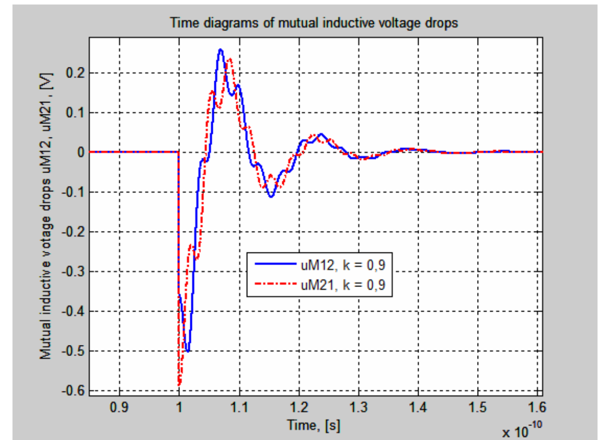

Fig. 13. Time diagrams of the mutual inductive voltage drops u_{M12} and u_{M21} at coefficient of magnetic connection $k = 0.9$

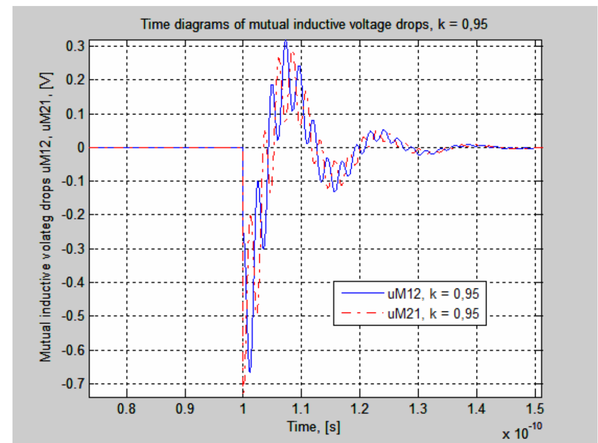

Fig. 14. Time diagrams of the mutual inductive voltage drops at coefficient of magnetic connection $k = 0.95$

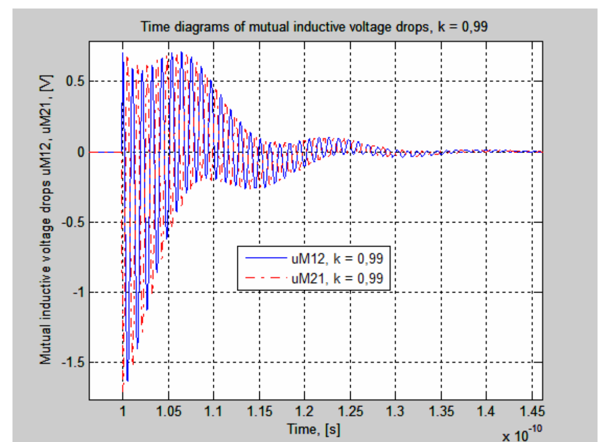

Fig. 15. Time diagrams of the mutual inductive voltage drops at coefficient of magnetic connection $k = 0.99$

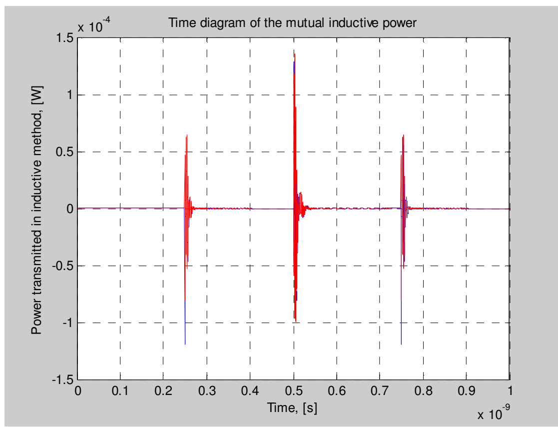

Fig. 16. Time diagram of the power transmitted by the electromagnetic induction at $f = 2\ GHz$ and $k = 0.9$

Another experiment that has been made is with the participation of rectangular voltage impulses with frequency of 20 GHz. The voltage drops across the memristors and the source voltages are presented in Fig. 17. The shape of the memristor voltage drops is very different from the ideal rectangular pulses of the source voltage but still there are no losses of information.

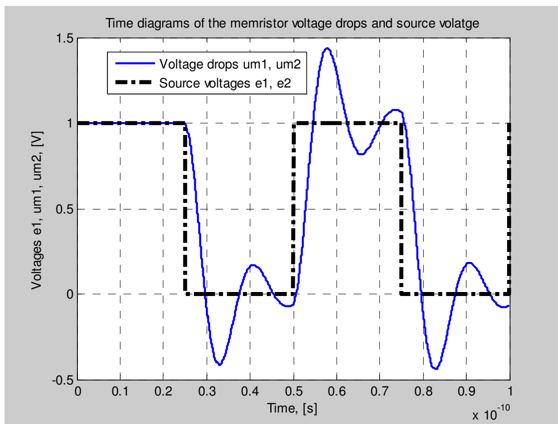

Fig. 17. Time diagrams of the source voltages and of memristors voltage drops at frequency *20 GHz* and coefficient of magnetic connection $k = 0.99$

The results for frequency of 200 GHz are presented in Fig. 18. In this case all the information is lost.

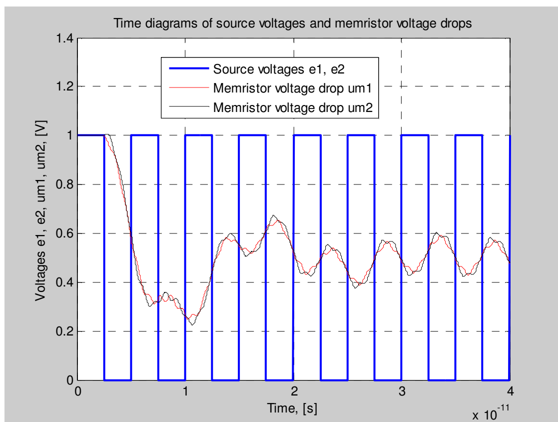

Fig. 18. Diagrams of source voltages and of memristor voltage drops at frequency *200 GHz* and coefficient $k = 0.99$

V. CONCLUSIONS

From the results presented above it is obvious that with increasing the frequency of the impulse sequence the parasitic parameters have strong influence on the impulse distortions. But for signals with frequencies up to 2 *GHz* these parameters do not have significant effect on the impulse signals. The tolerances of the memristor parameters have stronger influence on the memory matrix characteristics. Due to the effects of distorting of voltage impulses by parasitic capacitance and inductance of the memristor, the memristor voltage drop has front ricochet which is about 40 % of the magnitude of source pulse voltage. With increasing of the operating frequency of the signals the distortions of the pulses increases too. For frequencies up to 2 GHz the memristor works properly. For higher frequencies the distortions of the pulses are significant.

ACKNOWLEDGMENTS

The research results presented in the paper are financed from Contract № 121PD0072-08 for scientific projects for help of PhD Students of Scientific – research sector of Technical University – Sofia for 2012 - 2013 years.

REFERENCES

[1] Chua, L. O. Memristor – The Missing Circuit Element. IEEE Trans. on Circuit Theory, Vol. CT-18, pp. 507-519, September 1971.

[2] Pazienza, G. E., J. Albo-Canals. Teaching Memristors to EE Undergraduate Students. IEEE Circuits and Systems Magazine, pp. 36-44, 22 November 2011.

[3] Strukov, D. B., G. S. Snider, D. R. Stewart, R. S. Williams. The missing memristor found. Nature, doi:10.1038/nature06932, Vol 453, pp. 80 – 83,1 May 2008.

[4] Hayes, B. The memristor. Computing science, American Scientist, Volume 99, pp.106 – 110, 2011.

[5] Tour, J. M., T. He. The fourth element. Nature, Vol. 453, pp. 42 – 43, 1 May 2008

[6] Chua, L., S. Kang. Memristive devices and systems. Proceedings of the IEEE, Vol. 64, № 2, pp. 209 - 223, February 1976.

[7] Michelakis, K., T. Prodromakis, C. Toumazou. Cost-effective fabrication of nanoscale electrode memristors with reproducible electrical response. *Micro and nano letters, IET*, pp. 91 - 94, April 2010.

[8] Li, H., M. Hu. Compact model of memristors and its application in computing systems. EDAA, pp. 673 - 678, 2010.

[9] Strukov, D., R. S. Williams. Exponential Ionic Drift: fast switching and low volatility of thin-film memristors. Applied physics A, Materials Science and Processing, pp. 515 - 519, 2008.

[10] Xia, Q., W. Robinett, M. Cumbie et al. Memristor-CMOS Hybrid integrated Circuits for Reconfigurable Logic. *Nano letters*, Vol. 9, № 10, 2009.

[11] Haron, N., S. Hamdioui. On defect oriented testing for hybrid CMOS/memristor memory. IEEE Computer society, pp. 353 - 358, 2011.

[12] Torrezan, A., J. Strachan, G. Medeiros-Ribeiro, R. S. Williams. Sub-nanosecond switching of a tantalum-oxide memristor. Nanotechnology 22, pp. 1 - 7, November 2011.

[13] The Mathworks, Inc. SIMULINK – Dynamic system simulation for MATLAB, User Guide, version 3, January 1999.

[14] Zaplatilek, K. Memristor modeling in MATLAB & SIMULINK. Proceedings of the European Computing Conference, pp. 62 – 67.